Self-organized criticality in vector avalanche automata

Bruce McNamara* and Kurt Wiesenfeld
School of Physics, Georgia Institute of Technology, Atlanta, Georgia 30332
(Received 19 June 1989)

A new class of cellular automata is observed to evolve to a self-organized critical state. These "vector automata" obey a threshold relaxation condition that depends on the gradient of a scalar field, which is locally conserved except at the system boundaries. Both square and triangular lattices are studied and lead to virtually identical statistics; however, a particular (and natural) choice of boundary shape for the square lattice leads to trivial dynamics characteristic of a minimally stable configuration.

I. INTRODUCTION

Recently, there has been interest in a class of cellular automata that display "self-organized criticality," in which there are relaxation events of all sizes in the steady state.[1-6] These automata can be viewed as modeling spatially extended dynamical systems that obey a relaxational diffusion process when the system is locally stressed above some threshold value. The term "criticality" is used because the steady state is characterized by power-law spatial and temporal distributions typically associated with phase transitions of systems in thermal equilibrium. "Self-organized" refers to the fact that, after some transient period, the system *naturally evolves* into the critical state, without special adjustment of external parameters—that is, the critical state is an attractor of the dynamical system.

Because the specification of automaton rules are rather abstract compared with more traditional physical models, the elements of these rules have been described using the language of "sandpiles" and their induced avalanches, or of geophysical fault dynamics and their induced earthquakes.[7-11] Despite the fact that a recent experiment on granular flow[12] found no self-organized critical behavior, the theoretical interest in these models remains high. This is because our present understanding of dynamical systems having many degrees of freedom is poor; their importance lies in their relevance in describing spatially extended systems. Except in those cases where the essential dynamics can be reduced to a low-dimensional phase space, little is known about the general behavior of systems consisting of many degrees of freedom. In contrast to the great strides made for dynamical systems whose behavior is confined to a low-dimensional phase space, there are few examples of simple, recognizable behavior(s) common to large classes of systems. The discovery of self-organized criticality serves as a focal point for thinking about behavior which seems to require interplay among all degrees of freedom, and is therefore described by a very-large-dimensional phase space.

Though the first reports of self-organized criticality dealt with cellular automata (in which space, time, and the state variable are all discrete), it appears that the discrete nature of the state variable is not essential.[13] Moreover, an earthquake model[8] based on coupled ordinary differential equations exhibits qualitatively similar behavior, displaying events of all length scales up to the system size itself. It has also been argued that self-organized criticality can occur in a simple (nonlinear) partial differential equation.[14] These works are important because they may help to clarify the relationship between continuous ordinary and partial differential equations on the one hand and cellular automata on the other. While ordinary and partial differential equations are the mainstay of traditional physics, the computational convenience of cellular automata has made them a source of increased interest, for example, for their potential to simulate various fluid flows.[15,16]

In the wake of these several works, a few basic questions are emerging. The primary issue remains to identify those features which are essential for the generation of self-organized critical behavior. In this paper, we make a modest contribution to this question by studying a variation of the original automaton of Ref. 1 in two spatial dimensions. In order for the threshold condition to depend directly on the slope of the state variable $\psi(x,t)$, our threshold rule involves the vector-valued gradient of ψ. [Our original reason for doing this was to draw a closer analogy between our two-dimensional model and "real sand"; having said this, we do not think that such a correspondence is important viewed in the larger context.] Reduced to one dimension, the present models reduce to the original scalar automaton.[1]

As a vector-state automaton, the present system falls into a different class than models previously studied. This remark is meant in a physical sense rather than the more abstract sense of universality classes (i.e., the constancy of certain scaling exponents for distinct systems). Indeed, it is an open question whether the notion of universality is relevant to self-organized criticality. It turns out that the scaling exponents for the automata studied here differ from those in other works. Consequently, if universality is ultimately found to be relevant to self-organized critical systems, then the vector automata fall into a new universality class.

We study the dynamics using two different underlying

lattices, to test the effect on the global behavior. This is important since, if cellular automata are to be useful as models for macroscopic spatially extended systems, details at lattice length scales should vanish. We also explore the effect of different boundary shapes.

Our simulations show that the dynamics naturally evolve into a state characterized by avalanches of all sizes up to a cutoff that depends on the system size. We find that the avalanche size distribution is virtually identical for both square and triangular lattices; surprisingly, however, the choice of boundary shape in the square-lattice case can result in trivial dynamics characteristic of a minimally stable state.[1,17] We make a special effort to draw a connection between our rules and the direct discretization of partial differential equations (PDE's) (i.e., nonlinear diffusion equations). Besides introducing a more familiar way of thinking about these models, such PDE's can be amenable to certain theoretical analyses, as demonstrated by Hwa and Kardar, who used a renormalization-group approach to compute "critical exponents" characterizing the dynamics.[14]

We also found evidence that the critical state, though stationary only in the statistical sense, is surprisingly well ordered when viewed at the microscopic level. Moreover, we observe certain regularities in the way the critical state is formed: it appears to evolve from the system boundary inward. Though to date we have been unable to do so, it is possible that these empirical observations could be exploited to deduce the observed statistics of the critical state, and the manner in which correlations are built up from a (noncritical) initial state.

In Sec. II we define the rules for our model, and make the connection with a related nonlinear diffusion equation. The results of numerical simulations are presented in Sec. III, including some details of our numerical analysis. We end with a brief discussion in Sec. IV, and include some empirical observations concerning the nature of the statistical steady state.

II. RULES

In this section we define the rules governing our automata, and their relationship to a continuous diffusion equation. The rules are defined for two different spatial lattices, square and triangular.

It is helpful to begin with a physical picture that guides our choice of rules. We imagine a bounded two-dimensional surface (a table top); at each position on a discrete lattice, there is a number $\psi(x,y)$ (the height of the sandpile). At a randomly chosen site, we increase ψ by one unit

$$\psi(x,y)\rightarrow\psi(x,y)+1 , \tag{1}$$

which corresponds to dropping a grain of sand at position (x,y). We then check to see if the threshold condition is exceeded: in the present model, this condition depends on the local slope being greater than a threshold value (i.e., no sand flows unless the angle of repose is exceeded). If so, a relaxation rule is applied, corresponding to a diffusion of ψ. Since this relaxation may, in general, cause some neighboring site(s) to exceed threshold, the relaxation rule is applied repeatedly until all sites are quiescent, at which time another site is chosen at random for seeding.

In terms of a continuum picture, we have in mind a nonlinear diffusion equation

$$\partial_t\psi=\nabla\cdot\mathbf{J}(\nabla\psi)+\xi(t) , \tag{2}$$

where the current $\mathbf{J}$ is a nonlinear function of the gradient of ψ, and ξ is a weak (non-negative) random noise corresponding to the addition of sand, Eq. (1). The precise connection between $\mathbf{J}$ and the automaton will depend on the rules and the lattice, as we discuss below.

A. Square lattice

If the underlying lattice is square, we introduce the two slopes

$$S_x(x,y)=\psi(x+1,y)-\psi(x,y) , \tag{3a}$$

$$S_y(x,y)=\psi(x,y+1)-\psi(x,y) . \tag{3b}$$

If the addition of one unit to $\psi(x,y)$ causes either S_x or S_y (or both) to exceed the threshold magnitude S^*, the following relaxation rules are applied:

$$\begin{aligned}&\text{If } S_x(x,y)>S^*, \text{ then } \psi(x,y)\rightarrow\psi(x,y)+1,\ \psi(x+1,y)\rightarrow\psi(x+1,y)-1 ;\\ &\text{if } S_x(x,y)<-S^*, \text{ then } \psi(x,y)\rightarrow\psi(x,y)-1,\ \psi(x+1,y)\rightarrow\psi(x+1,y)+1 ;\end{aligned} \tag{4a}$$

$$\begin{aligned}&\text{if } S_y(x,y)>S^*, \text{ then } \psi(x,y)\rightarrow\psi(x,y)+1,\ \psi(x,y+1)\rightarrow\psi(x,y+1)-1 ;\\ &\text{if } S_y(x,y)<-S^*, \text{ then } \psi(x,y)\rightarrow\psi(x,y)-1,\ \psi(x,y+1)\rightarrow\psi(x,y+1)+1 .\end{aligned} \tag{4b}$$

In words, for each slope that is above threshold, one unit of ψ is transferred "downhill." If both S_x and S_y exceed threshold simultaneously, then relaxation takes place in both directions simultaneously, so that $\psi(x,y)$ diminishes by two units. The boundary conditions are that ψ is zero on the system's perimeter.

If we use the notation that $\nabla\psi=(S_x,S_y)$, then one can represent the above rules in terms of a discretized version of Eq. (2) with the current $\mathbf{J}$ given by

$$\mathbf{J}=(D[S_x],D[S_y]) \tag{5}$$

and

$$\nabla\cdot\mathbf{J}=J_x(x,y)-J_x(x-1,y)+J_y(x,y)-J_y(x,y-1) , \tag{6}$$

where $D[u]$ is the nonlinear operator that takes the in-

teger part of its argument after dividing by (S^*+1): $D[u]=\mathrm{Int}[u/(S^*+1)]$. (The critical slope S^* is the natural unit of slope in these models; recall that S^* is the largest stable slope.) In our simulations, the quantity $D[u]$ only achieves the values of -1, 0, or $+1$. Thus, according to the classification of Ref. 6, this is a "local, limited model."

B. Triangular lattice

Each site in this lattice has six nearest neighbors; the coordinate system (x,y) for a point on this lattice is indicated in Fig. 1. It is convenient to introduce three coordinate axes, and to define the three slopes S_x, S_y, and S_z,

$$S_x(x,y)=\psi(x+1,y)-\psi(x,y)\ , \tag{7a}$$

$$S_y(x,y)=\psi(x,y+1)-\psi(x,y)\ , \tag{7b}$$

$$S_z(x,y)=\psi(x+1,y+1)-\psi(x,y)\ . \tag{7c}$$

Of course, only two of these are independent; in the continuum problem this is expressed by the condition that $\nabla\times\mathbf{S}=0$, since $\mathbf{S}$ is the gradient of a scalar field ψ. In our discrete model, it is easy to see that the condition

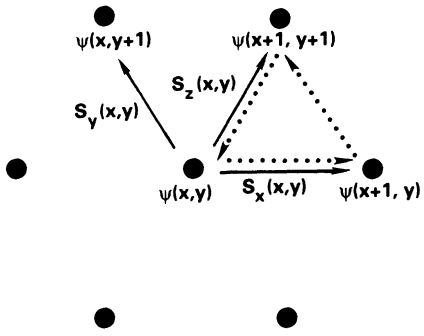

FIG. 1. Coordinate system for the triangular lattice. The slopes evaluated around the dotted path obey the "zero-curl" constraint Eq. (8).

linking the S_k may be expressed by (see Fig. 1)

$$S_x(x,y)+S_y(x+1,y)-S_z(x,y)=0\ . \tag{8}$$

The relaxation rules for S_x and S_y are the same as before [Eq. (4)], but with the additional rule for S_z,

$$\begin{aligned}&\text{If } S_z(x,y)>S^*,\ \text{then } \psi(x,y)\to\psi(x,y)+1,\ \psi(x+1,y+1)\to\psi(x+1,y+1)-1\ ;\\ &\text{if } S_z(x,y)<-S^*,\ \text{then } \psi(x,y)\to\psi(x,y)-1,\ \psi(x+1,y+1)\to\psi(x+1,y+1)+1\ .\end{aligned} \tag{9}$$

As before, we can represent these rules as the discretized version of the nonlinear diffusion equation with current $\mathbf{J}$; here,

$$\mathbf{J}(D[S_x],D[S_y],D[S_z])\ , \tag{10}$$

using three coordinates. In terms of the two independent coordinates x and y, this can be written [with the use of Eq. (8)]

$$\mathbf{J}=(D[S_x(x,y)]+D[S_x(x,y-1)+S_y(x+1,y-1)],D[S_y(x,y)]+D[S_x(x,y)+S_y(x+1,y)])\ . \tag{11}$$

Note that, in contrast to the square lattice expression (5), the x component of the current depends on the slope in the y direction. This can have important consequences for the observed dynamics, as will be discussed in Sec. IV.

Finally, as with the square lattice, the boundary conditions are that $\psi(x,y)=0$ on the system's perimeter.

III. RESULTS

We ran simulations for both the square and triangular lattices. In order to insure that the data represented steady-state behavior, we started from a state known (by experience) to be close to the statistical steady state, and then ran the dynamics for a large number of grains (10 000–75 000, depending on the size of the system) before starting to take histogram data. We checked that this gives data that are repeatable and in agreement with data taken when the system is allowed to build up "from scratch" [i.e., initial condition $\psi(x,y)=0$ everywhere].

As discussed more fully in Sec. IV, we have observed empirically that the steady-state automaton is characterized by a pyramid-shaped "sandpile" whose sides have a slope equal to S^* minus 0.5. (Recall that S^* is the largest *stable* slope.) In order to minimize the time required to reach a steady state, the initial state was set to be a pyramid with precisely this slope. Typically, between 200 000 and 1 000 000 grains were used for each histogram. Runs using a larger number of grains made little difference except to extend the histogram out to the largest flip numbers. The critical slope was taken to be 4 for the square lattice and 6 for the triangular lattice, i.e., equal to the number of nearest neighbors. Note that any value of S^* larger than these will not affect the steady-state dynamics (for these boundary conditions).

After each loading of a site, the resulting relaxation rules are applied until no slopes are above threshold. The entire relaxation event can be characterized in a number of ways; in what follows we will focus on the *flip number* F and the *event duration* t. The flip number—also called the cluster size in Ref. 1—is the total number of sites which exceed the threshold condition at some instant during the event: if a site is triggered m distinct times during a single event, it is counted m times. (Thus it is possible for F to exceed the total number of lattice points

in the system.) The main reason for focusing on F is that it spans a larger range than, say, the "drop number," which is the number of grains that exit the boundary. Since we are limited to relatively small systems as a practical matter, F is the more attractive quantity. The event duration t is simply the number of iterations the relaxation rule must be applied to bring all slopes below threshold.

In collecting the histograms, one finds a great deal of scatter for the largest events. This is a simple matter of statistics: there may be many large avalanches, but only a small number with have, say, precisely $F=1021$. Thus one is faced with a choice of binning procedure to smooth the data. We chose to smooth by averaging bins within 10% of each given avalanche size F. That is, if $P(F)$ is the raw histogram (normalized by the total number of grains dropped), we formed the smoothed avalanche distribution $\bar{P}(F)$, where

$$\bar{P}(F)=A\left[\sum_{F'=F_L}^{F_U} P(F')+P(F_L-1)(F_L-F/\gamma)+P(F_U+1)(F\gamma-F_U)\right],$$

where

$$F_L=\mathrm{Int}(1+F/\gamma),\quad F_U=\mathrm{Int}(F\gamma),$$

$$A=(F\gamma-F/\gamma+1)^{-1},$$

and the constant γ is 1.10 for averaging over bins within 10% of F. The final two terms represent fractional parts of the bins at the lower and upper limits of the sum. The precise value of γ was not found to be crucial; the virtue of this procedure is that it has its largest bins where the data are most sparse.

We begin with the results obtained for the square lattice, governed by the relaxation rules Eq. (4). Interestingly, the behavior is completely different for the two different choices of boundary conditions that we studied.

If the boundary is a square of side L, with sides running parallel to the lattice vectors (so that both x and y range from 1 to L), the stationary state is extremely simple. We always chose L odd so that the system has a unique central site. Specifically, the system builds up to a (square based) pyramid, with ridges along the main diagonals and apex at the center. On each of the four faces, either $S_x=S^*$ and $S_y=0$ or vice versa. Once in this state, the addition of a single grain at (x,y) induces a slide in which one, two, or four grains tumble all the way to the boundary, depending on whether (x,y) is on a face, a ridge, or the apex, respectively. Except for the loaded site, the entire pile remains unchanged. (Strictly speaking, there are exceptional sites on the ridges and apex which temporarily become subthreshold. But these sites represent a vanishingly small fraction of sites with increasing system size.) It is a straightforward matter to compute the avalanche distribution explicitly: one finds that, up to the normalization constant $1/L^2$,

$$P(F)=\begin{cases} L-\frac{1}{4}, & F=0 \\ 4L-8F, & F\le\dfrac{L-1}{2},\ \text{odd} \\ 4L-8F+2, & F\le\dfrac{L-1}{2},\ \text{even} \\ 2, & \dfrac{L-1}{2}<F\le L-1,\ F\ \text{even} \\ \frac{1}{4}, & F=2L+2 \\ 0, & \text{otherwise}. \end{cases} \tag{12}$$

The behavior of this system is reminiscent of the minimally stable state achieved by the one-dimensional version of the automaton originally introduced by Bak, Tang, and Wiesenfeld.[1] In particular, a perturbation at any site leads to an avalanche extending to the system's edge, yet the state of the system is virtually unchanged after each event.

The constant contributions that appear for F even and for $F=2L+2$ vanish in the large-L limit, corresponding to the fact that the fraction of ridge and apex sites becomes negligible. In this limit, $\bar{P}(F)$ is a straight line (up to the cutoff at $L/2$) with slope that diminishes with F; asymptotically, this slope tends to zero. Thus one might view the $L\to\infty$ limit as a power law $\bar{P}(F)\sim F^{\tau}$, with $\tau=1$, but with diminishing amplitude. Nevertheless, we view this behavior as fundamentally different from other measured distributions for self-organized criticality, which are characterized by a negative exponent. The notion that $\tau=1$ is somehow a special case is reinforced by the fact that a change in boundary shape leads to the more typical power law with negative exponent, as we now discuss.

The other boundary shape we chose for the square lattice was also a square, but with sides inclined at 45° with respect to the lattice vectors: we call this the "diamond" boundary. Thus, if we specify the diamond to have side of length L, there is a total of $L^2+(L-1)^2$ sites, and the coordinates are bounded by the four conditions

$$x+y=L,\quad x-y=L,\quad y-x=L,\quad x+y=3L\ . \tag{13}$$

For this boundary the system builds up *only roughly* to a pyramid, with measured avalanche distribution shown in Fig. 2. Clearly, one observes much larger events than previously; viewed as a function of increasing L, one sees some limiting function "unfold." The observed distributions are consistent with a power law $\bar{P}(F)\sim F^{-\tau}$, with $\tau=1.4$. The roll off at the largest avalanche sizes is due to finite-size effects: the point at which the curve breaks moves out as a function of increasing system size. Figure 3 shows the histogram for the event duration t. As is typical, the data does not span as many decades as that for the flip number, even if we go to a larger system size. Nevertheless, the data fit a power law tolerably well, $\bar{P}(t)\sim t^{-\alpha}$, with $\alpha=1.6$.

Finally, we turn to the triangular lattice, governed by the relaxation rules Eqs. (4) and (9). We chose a hexagonal boundary with sides parallel to the lattice vectors, and having main diagonal d. In contrast to the square lattice, this "commensurate" situation did not lead to

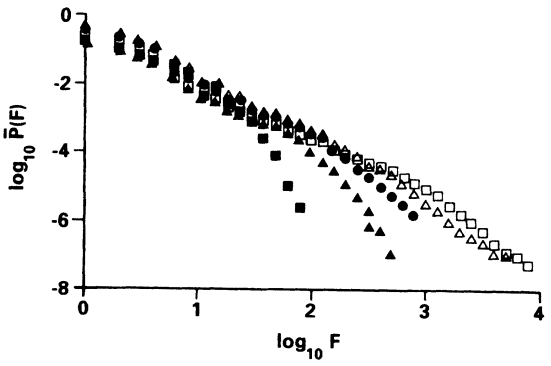

FIG. 2. Flip number probability density $\bar{P}(F)$ for the square lattice with diamond-shaped boundary of side L, for $L=8$ (closed squares), $L=16$ (closed triangles), $L=32$ (closed circles), $L=64$ (open triangles), and $L=128$ (open squares). In each case, the distribution reflects a total of at least 200 000 avalanches.

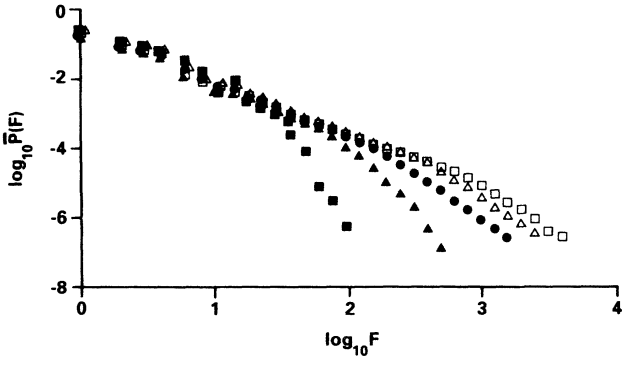

FIG. 4. Avalanche size distribution $\bar{P}(F)$ for the triangular lattice, with hexagon-shaped boundary with main diagonal d, for $d=16$ (closed squares), $d=32$ (closed triangles), $d=64$ (closed circles), $d=128$ (open triangles), and $d=256$ (open squares). Each curve represents a total of at least 200 000 avalanches.

trivial steady-state dynamics. In fact, the avalanche distribution $\bar{P}(F)$ is virtually identical to that of the square lattice with diamond boundary, as is evident from a comparison of Figs. 2 and 4. Indeed, when these two figures are superimposed, they appear to form a single data set; even the oscillations for smallish avalanches (not apparent on the scale of the figures) match up. The only question is how to quantitatively compare the sizes of the two distinct geometries. The natural choice is to use the total number of lattice sites—i.e., the area. Thus, for the hexagon with main diagonal d, the area is $N=(3d^2+1)/4$, and for the diamond of side L, the area is $N=2L^2-2L+1$. Indeed, viewed as a sequence of curves with increasing N, these appear to unfold a unique $N\rightarrow\infty$ limiting distribution. The event duration data show the same compatibility between lattice types as for the flip number, so we have chosen to omit the plot of $\bar{P}(t)$ for the triangular lattice.

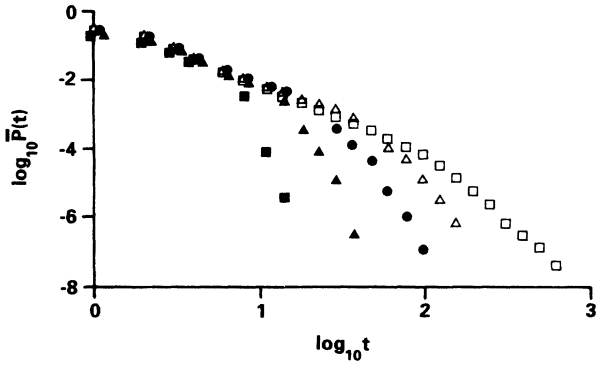

FIG. 3. Event duration probability density $\bar{P}(t)$ for the square lattice with diamond-shaped boundary of side L, for $L=8$ (closed squares), $L=16$ (closed triangles), $L=32$ (closed circles), $L=64$ (open triangles), and $L=256$ (open squares). In each case, the distribution reflects a total of at least 200 000 avalanches.

We also ran simulations for the triangular lattice with a triangular-shaped boundary, and found results statistically identical to those for the hexagonal boundary. That is, the occurrence of trivial dynamics was never observed for the triangular lattice. As discussed below, we believe that the presence of trivial dynamics in the square lattice is an artifact of the severe anisotropy of the fourfold coordination number; sixfold coordination seems sufficient to eliminate the possibility of trivial steady-state dynamics.

IV. DISCUSSION

Our simulations show that the "vector threshold" automaton displays the earmarks of self-organized criticality. Virtually identical stationary state statistics are obtained for two different underlying lattices, as one would expect for processes which involve events having length scales up to the system size itself. Interestingly, however, the choice of boundary shape profoundly affects the dynamics of the square lattice: specifically, a quite "natural" choice of a square with boundary edges parallel to the lattice vectors leads to trivial dynamics. The system evolves to a pyramidal shape; the surface $\psi(x,y)$ is as perfect (i.e., nonstatistical) as possible considering the presence of a random seeding rule. This is the minimally stable state for this dynamics, since the addition of one unit anywhere induces an avalanche. The avalanche dynamics correspond to that of the minimally stable state described in the one-dimensional (scalar) automaton of Ref. 1. This is not too surprising insofar as the vector automaton reduces to the original scalar model in one dimension.

Can we understand why the square lattice can behave "trivially" for this choice of boundary, while the triangular lattice does not? We can gain some insight by noting an analogous situation that arises in the study of lattice-gas automata.[15–16] There, deterministic collision rules on a square lattice lead to special (and undesirable) dynamics, due to the existence of an extra conserved quanti-

ty which is not present for the triangular lattice. In fact, we can identify an "extra" conserved quantity in our automaton for the square lattice, as follows. If we take the gradient of Eq. (2), we get

$$\partial_t S_x = \partial_x[\nabla\cdot\mathbf{J}(\nabla\psi)] + \partial_x \xi(t) ,$$
$$\partial_t S_y = \partial_y[\nabla\cdot\mathbf{J}(\nabla\psi)] + \partial_y \xi(t) . \quad (14)$$

For the pyramid state, either S_x or S_y is zero over an entire face, with the result that the two slope equations decouple; the zero slope stays zero during the entire relaxation event. For the triangular lattice, this decoupling cannot occur, as can be seen from the "cross-coupled" expression for the current Eq. (11); if either S_x or S_y is above threshold, this induces a change in both S_x and S_y. In the case of the square lattice with diamond boundaries, the coupling between S_x and S_y occurs through the boundary conditions rather than the local current. This can be observed directly by watching a simulation in progress: the pyramid formation begins at the boundary, and works in toward the center with time.

Of course, this discussion does not reveal *why* the system should be attracted to the pyramid state in the first place; rather, it shows why once in the pyramid state, it will remain there.

While working with these automata we observed that even the nontrivial (statistical) critical states were remarkably more ordered than the broad avalanche distribution might suggest. Invariably, the steady state was marked by a "macroscopic" slope—the average slope over an entire face of the pyramid— that was well defined even on the smallest length scales, and which changed very little with time. If we define the row r of a site to be its distance from the nearest boundary, then the probability distribution of the heights $\psi(r)$ is centered about

$$\psi_0(r) = S_m r + b ,$$

where the macroscopic slope S_m is empirically observed to be equal to $S^* - 0.50$. The constant b is measured to be 1.1 for the square lattice and 0.7 for the triangular lattice. Aside from a very slight deviation for sites within a few rows of the boundary or the apex, the data are in excellent agreement with this rule. Furthermore, the width of the distribution of $\psi(r)$ does not increase with r, rather it remains fixed at roundly a few bins to either side of $\psi_0(r)$. It may be that this observation can be used to construct a theory for the distribution of avalanches, perhaps calculating the power-law exponent for the flip number distribution $\bar{P}(F)$. As yet no work has been done in this direction.

There are three important issues that we have not addressed here. The first is that, given that a system evolves into a self-organized critical state, what is the best way to characterize the statistical behavior? Kadanoff *et al.*[6] have suggested that a multifractal description may be more appropriate than the more traditional finite-size-scaling analysis. We have compared these two descriptions for our data, and find no distinct preference for one over the other: both work tolerably well, though neither gives an outstanding fit. The second issue, which to our mind is more fundamental, is whether or not self-organized criticality requires a locally conserved quantity.[13,14,18–20] In Ref. 14, it was suggested that the existence of a locally conserved quantity is responsible for the resulting criticality in their study of a nonlinear partial differential equation; in contrast, very recent work on cellular automata has suggested that this is not a necessary ingredient.[18–20] The models studied in this paper have a relaxation rule which manifestly conserves ψ locally (except, of course, at the boundaries). This is reflected by the continuity equation (2), and the resulting dynamics unambiguously reveals self-organized critical behavior. An interesting extension of the present work would be to alter the local rules in a way that breaks the local conservation, and see the degree to which criticality is maintained. The third point is the issue of universality, that is, whether the exponents quantitatively agree for different automata. The present model gives $\tau = 1.4$ and $\alpha = 1.6$, whereas in Ref. 1 $\tau = 1.0$ and $\alpha = 0.43$. Of the four two-dimensional models studied in Ref. 6, two values of τ are inconsistent with the value measured here, and agreement with the other two is uncertain ($\tau = 1.35$ and $\tau = 1.5$, unfortunately no values of α were reported). Our own opinion is that universality in this sense may not be relevant for these systems.

Finally, we have taken pains to draw a correspondence between the automaton rules and partial differential equations. One reason is our hope that such analogies will prove useful for gaining insight into these nonlinear diffusion processes. In addition, existing methods for extracting quantitative information proceed from the continuum limit:[14] in particular, it is a challenge to see if renormalization-group methods can correctly compute the exponents we have arrived at by purely numerical means. It may also be that our empirical observations regarding the remarkable microscopic regularity of the critical state can be exploited to gain insight into the origin of self-organized criticality, and to compute quantities characterizing the macroscopic statistical behavior.

ACKNOWLEDGMENTS

We thank Geza Gyorgyi, Chao Tang, and Andy Zangwill for stimulating discussions. This research was supported in part by the Office of Naval Research under Contract No. N00014-88-K-0494.

*Permanent address: Department of Physics, Reed College, Portland, OR 97202.

[1] P. Bak, C. Tang, and K. Wiesenfeld, Phys. Rev. Lett. **59**, 381 (1987); Phys. Rev. A **38**, 364 (1988).

[2] C. Tang and P. Bak, Phys. Rev. Lett. **60**, 2347 (1988); J. Stat. Phys. **51**, 797 (1988).

[3] P. Bak and C. Tang, Phys. Today **42**, S27 (1989).

[4] K. Wiesenfeld, C. Tang, and P. Bak, J. Stat. Phys. **54**, 1441

(1989).
[5]P. Alstrom, Phys. Rev. A **38**, 4905 (1988).
[6]L. P. Kadanoff, S. R. Nagel, L. Wu, and S.-M. Zhou, Phys. Rev. A **39**, 6524 (1989).
[7]H. Takayasu and M. Matsuzaki, Phys. Lett. **131**, 244 (1988).
[8]J. M. Carlson and J. S. Langer, Phys. Rev. Lett. **62**, 2632 (1989).
[9]P. Bak and C. Tang (unpublished).
[10]K. Ito and M. Matsuzaki (unpublished).
[11]A. Sornette and D. Sornette, Europhys. Lett. **9**, 197 (1989).
[12]H. M. Jaeger, C.-H. Liu, and S. R. Nagel, Phys. Rev. Lett. **62**, 40 (1989).
[13]Y. Zhang, Phys. Rev. Lett. **63**, 470 (1989).
[14]T. Hwa and M. Kardar, Phys. Rev. Lett. **62**, 1813 (1989).
[15]U. Frisch, B. Hasslacher, and Y. Pomeau, Phys. Rev. Lett. **56**, 1505 (1986).
[16]U. Frisch, D. D'Humieres, B. Hasslacher, P. Lallemand, Y. Pomeau, and J. P. Rivet, Complex Syst. **1**, 649 (1987).
[17]C. Tang, K. Wiesenfeld, P. Bak, S. Coppersmith, and P. Littlewood, Phys. Rev. Lett. **58**, 1161 (1987).
[18]P. Bak, K. Chen, and M. Creutz (unpublished).
[19]P. Bak, K. Chen, and C. Tang (unpublished).
[20]K. Chen and P. Bak (unpublished).